Journal of Crystal Growth 323 (2011) 466–469

Contents lists available at ScienceDirect

Journal of Crystal Growth

journal homepage: www.elsevier.com/locate/jcrysgro

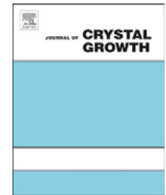

The transition mechanisms of type-II GaSb/GaAs quantum-dot infrared light-emitting diodes

Chi-Che Tseng [a], Wei-Hsun Lin [a], Shung-Yi Wu [a], Shu-Han Chen [b], Shih-Yen Lin [b,c,d,*]

[a] *Institute of Electronics Engineering, National Tsing Hua University, Hsinchu, Taiwan*
[b] *Research Center for Applied Sciences, Academia Sinica, Taipei, Taiwan*
[c] *Department of Photonics, National Chiao-Tung University, Hsinchu, Taiwan*
[d] *Institute of Optoelectronic Sciences, National Taiwan Ocean University, Keelung, Taiwan*

ARTICLE INFO

Available online 27 October 2010

Keywords:
B1. Antimonides
B3. Light emitting diodes

ABSTRACT

The light-emitting diode (LED) with a single GaSb QD layer embedded in a GaAs n–i–p structure operated under different injection currents and temperatures is investigated. With increase in injection currents, room-temperature electroluminescence (EL) peak blue shift is observed until a saturation of EL intensity is reached. In the temperature-varying EL measurements, with increase in temperatures, EL peak blue shift and then red shift are observed, which is attributed to the enhanced luminescence of the smaller QDs with increase in temperatures lower than 100 K. The understanding of the operation mechanisms for the device is advantageous for the practical application of type-II LEDs.

© 2010 Elsevier B.V. All rights reserved.

1. Introduction

Quantum-dot (QD) light-emitting devices operated in the near infrared range have been widely investigated in recent years [1–4]. Due to its unique optical characteristics, high-power and temperature-insensitive QD laser diodes (LDs) have already been fabricated [1,2]. To push the emitting wavelengths to the optical-communication range, device/structure with self-assembled InAs QDs capped by an InGaAs strain-reducing layer has exhibited 1.3 μm emitting wavelength [3]. With the incorporation of Sb atoms, even longer emitting wavelength 1.55 μm is observed for InAs QDs grown on GaAsSb barrier layers [4]. However, for such a QD structure with type-I band alignment, it is difficult to achieve even longer emitting wavelengths due to limited choices in barrier materials. Therefore, GaSb QDs with type-II band alignment has provided an alternate choice for the fabrication of infrared light-emitting devices based on QD structures. Compared with the type-I InAs QD structures, the main advantage of the GaSb QD structure is the wide barrier choice from GaAs to GaAsSb and even InGaP. The choice of different barriers may provide even longer emitting wavelengths for the devices based on this QD structure. In previous reports, despite its type-II alignment, photoluminescence (PL) are already observed for GaSb/GaAs QDs [5,6]. A light-emitting diode (LED) based on the type-II GaSb/GaAs QD structure operated at room temperature has also been demonstrated elsewhere [7]. To further understand the operation mechanisms of the device, detailed investigation is still required. In this paper, the LED with a single GaSb QD layer embedded in a GaAs n–i–p structure operated under different injection currents and temperatures is investigated.

2. Experimental

The GaSb QD LED sample discussed in this paper is prepared by the Riber Compact 21 solid-source molecular beam epitaxy (MBE) system. With the (1 0 0)-oriented semi-insulating GaAs substrate, a single 3.0 monolayer (ML) GaSb QD layer are embedded in the GaAs n–i–p structure. The growth procedure for the sample is a 300 nm GaAs bottom contact layer p-type doped to 2×10^{18} cm^{-3} grown at 580 °C, a 200 nm undoped GaAs layer grown at 580 °C, a 3.0 ML GaSb QD layer grown at 490 °C with V/III ratio ~1.3, a 200 nm undoped GaAs layer grown at 580 °C and a 300 nm GaAs top contact layer n-type doped to 2×10^{18} cm^{-3} grown at 580 °C. The pre- and post-Sb soaking times adopted for the sample are 15 and 120 s, respectively. Standard photolithography and wet chemical etching are adopted to fabricate the devices with 450×630 μm^2 mesas. For light extraction, grid top contact is adopted. The positive and negative biases of measurements are defined according to the voltages applied to the top contact of the devices. The Keithley 2601A system is used as the continuance and pulse current source. The PL, μ-PL and EL spectra are observed by using a Jobin Yvon's NanoLog3 system with an InGaAs detector cooled by liquid nitrogen.

* Corresponding author at: Research Center for Applied Sciences, Academia Sinica, 128 Section 2, Academia Road, Nankang, Taipei 11529, Taiwan.
Tel.: +886 3 5744364; fax: +886 3 5734217.
E-mail address: shihyen@gate.sinica.edu.tw (S.-Y. Lin).

0022-0248/$ - see front matter © 2010 Elsevier B.V. All rights reserved.
doi:10.1016/j.jcrysgro.2010.10.109

3. Results and discussion

The room-temperature PL and EL spectra of the device measured with laser pumping power density 0.9 W/cm^2 and pulse forward injection current 1.0 mA are shown in Fig. 1(a). The duty cycle is 5% and the operation frequency is 1 kHz. As revealed in the figure, similar PL and EL spectra curves with two peaks 1.09 and 1.20 eV are observed, which suggests that the same transition mechanisms are responsible for the two spectra. In previous publications, the PL spectra of the GaSb QDs are mostly observed at low temperature [5,6]. One possible mechanism responsible for this phenomenon may be the dislocations produced in the Sb/As interfaces such that only luminescence at low temperature could be observed. Therefore, the observation of significant PL and EL signals at room temperature suggests that improved Sb/As interfaces with low defect densities are obtained for the sample with the additional pre- and post-Sb soaking procedure. To investigate the transition mechanisms responsible for the two peaks, normalized PL and μ-PL spectra measured under pumping power densities 0.9 and 1×10^3 W/cm^2 are shown in Fig. 1(b). As revealed in the figure, the two peaks are observed in both spectra, while different dominant peaks with lower energy in the PL spectrum and higher energy in the μ-PL spectrum are obtained. The phenomenon is attributed to the state-filling effect frequently observed for InAs QDs. We would therefore attribute these two peaks to ground- and excited-state luminescence, which correspond to the transitions between the ground state in the GaAs triangular well to the ground and excited state in the GaSb QD, respectively [9]. Also revealed in the figure is the blue shift of the peaks under a higher pumping power density, which suggests that type-II transitions are responsible for the luminescence [7–9].

The EL spectra of the device measured under different pulse forward injection currents, which ranges from 1 to 20 mA are shown in Fig. 2. The duty cycle is 5% and the operation frequency is 1 kHz. As shown in the figure, when the device is under low injection currents, both ground and excited luminescence are clearly observed. With increase in injection currents, EL peak blue shift and intensity enhancement are observed. However, by further increase in the injection currents, the EL intensities would saturate and the EL peaks would remain unchanged. The phenomenon is more pronounced for the ground-state luminescence. Also observed in the figure is the appearance of an additional peak at ~1.38 eV between the GaAs bandgap and excited-state luminescence at higher injection currents. The peak is attributed to the luminescence of the GaSb wetting layer (WL)/GaAs type-II interface [10]. Since the device structure is of n–i–p diode, the forward current would flow through the GaSb WL/GaAs interface before reaching the GaSb QDs/GaAs interface. Therefore, although most of the carriers would tend to accumulate at the GaSb QDs/GaAs interfaces, weak luminescence would still be observed under higher injection conditions.

The EL intensity/injection current ratios and EL peak energies versus the third root of the injection currents for the ground-state luminescence are shown in Fig. 3. As shown in the figure, when the device is under low injection currents, the EL peak energies are linearly dependent with the third root of the injection currents, which is frequently observed for type-II luminescence [7,11]. Detail results have been discussed elsewhere [7]. However, when the EL intensity/injection current ratio begins to decrease at ~5 mA, the EL peak energy would gradually become unchanged. The results suggest that there is an upper limit to the optical recombination

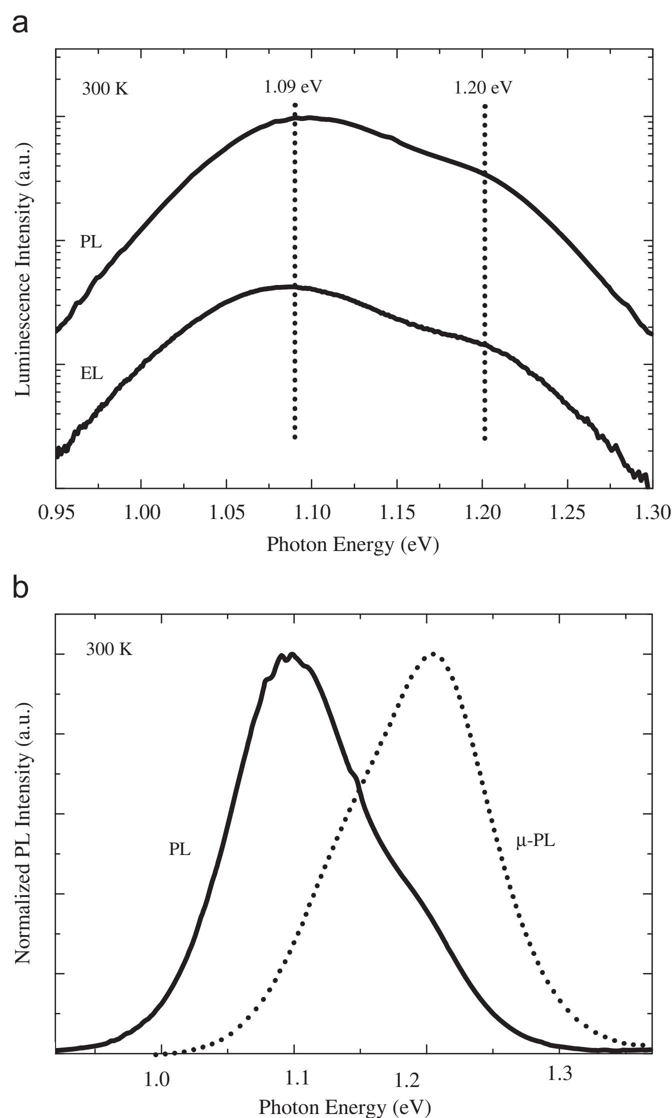

Fig. 1. (a) Room-temperature PL and EL spectra and (b) normalized PL and μ-PL spectra of the device.

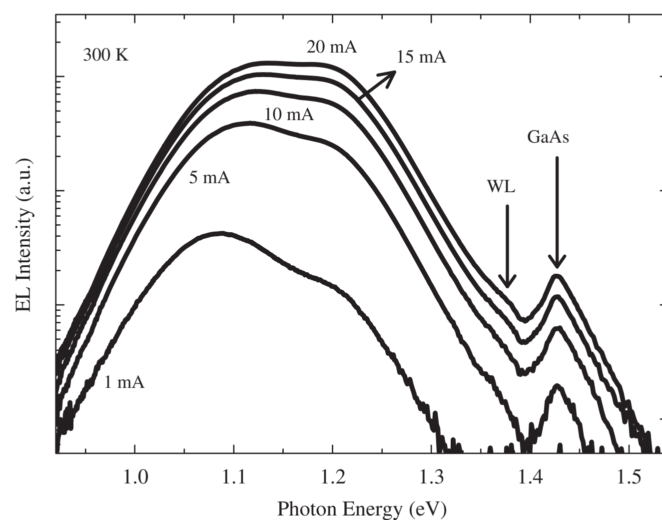

Fig. 2. EL spectra of device measured under different pulse forward injection currents ranging from 1 to 20 mA. The duty cycle is 5% and the operation frequency is 1 kHz.

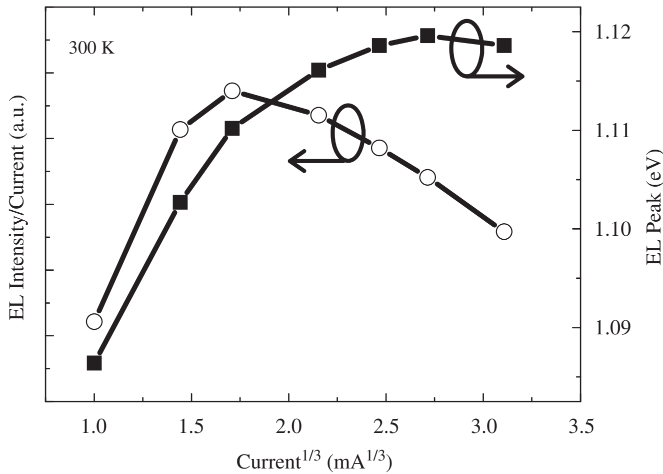

Fig. 3. EL intensity/injection current ratios and EL peak energies versus the third root of the injection currents for the ground-state luminescence.

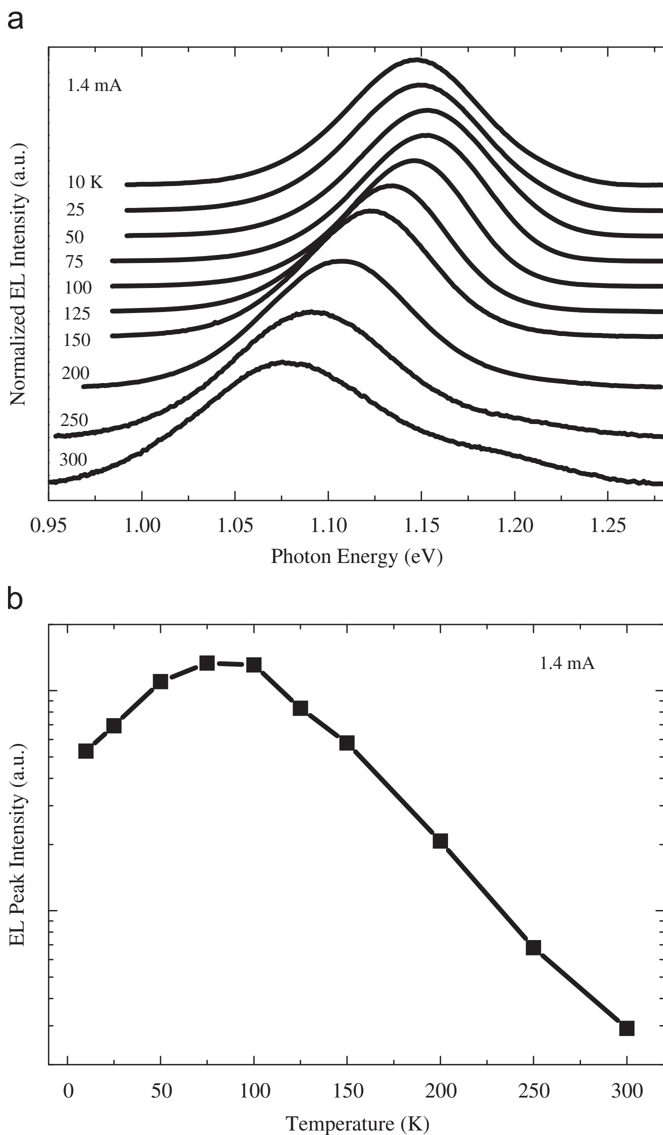

Fig. 4. (a) EL spectra of LED measured under different temperatures and (b) EL peak intensities of device measured under different temperatures with fixed constant forward injection current 1.4 mA.

efficiency of the injection currents. The results would also limit the performances of the LED. To further enhance the device efficiency, additional carrier confinement schemes should be adopted in the future.

The EL spectra of the LED measured under different temperatures with fixed constant forward injection current 1.4 mA are shown in Fig. 4(a). As revealed in the figure, when the measurement temperature is below 75 K, the ground-state luminescence blue shift is observed with increase in measurement temperatures. However, when the temperature is higher than 75 K, EL peak red shift is observed. To investigate this phenomenon, the EL peak intensities of the device measured under different temperatures are shown in Fig. 4(b). The EL intensity would increase with increase in temperature until 100 K. For the measurement temperature higher than 100 K, the EL intensities would decrease with increase in temperatures. This phenomenon suggests that when the temperature is lower than 100 K, the influence of phonons with increase in temperatures is not significant for the carrier lifetime in the GaSb QDs. Therefore, with increase in temperatures, holes confined in larger GaSb QDs would be thermally activated such that the carrier transport to the nearby smaller dots via the wetting layer would become possible. In this case, hole distribution in the QDs would become more uniform such that optical recombination processes would increase under the same injection condition. The results would be an increase in EL intensity and peak blue shift with increase in temperatures. For the temperature higher than 100 K, the bandgap shrinkage and intense electron–phonon interaction would result in EL peak red shift and intensity reduction.

4. Conclusions

In conclusion, the LED with a single GaSb QD layer embedded in a GaAs n–i–p structure operated under different injection currents and temperatures is investigated. The results obtained under different injection currents suggest that there is an upper limit to the optical recombination efficiency for the LED. To enhance the device performances, an additional carrier confinement schemes are required in the future. In the temperature-varying EL measurements lower than 100 K, the device has exhibited a unique optical characteristic of increase in EL intensity and peak blue shift with increase in temperatures. The understanding of the operation mechanisms for the device is advantageous for the practical application of type-II LEDs.

Acknowledgment

This work was supported in part by the National Science Council, Taiwan under grant nos. NSC 99-2628-E-001-001 and NSC 99-2911-I-001-010.

References

[1] Q. Cao, S.F. Yoon, C.Y. Liu, C.Y. Ngo, Nanoscale Res. Lett. 2 (2007) 303.
[2] S.S. Mikhrin, A.R. Kovsh, I.L. Krestnikov, A.V. Kozhukhov, D.A. Livshits, N.N. Ledentsov, Yu.M. Shernyakov, I.I. Novikov, M.V. Maximov, V.M. Ustinov, Zh.I. Alferov, Semicond. Sci. Technol. 20 (2005) 340.
[3] W.S. Liu, H. Chang, Y.S. Liu, J.I. Chyi, J. Appl. Phys. 99 (2006) 114514.
[4] H.Y. Liu, Y. Qiu, C.Y. Jin, T. Walther, A.G. Cullis, Appl. Phys. Lett. 92 (2008) 111906.
[5] G. Balakrishnan, J. Tatebayashi, A. Khoshakhlagh, S.H. Huang, A. Jallipalli, L.R. Dawson, D.L. Huffaker, Appl. Phys. Lett. 89 (2006) 161104-1.
[6] M.C. Lo, S.J. Huang, C.P. Lee, S.D. Lin, S.T. Yen, Appl. Phys. Lett. 90 (2007) 243102.
[7] S.Y. Lin, C.C. Tseng, W.H. Lin, S.C. Mai, S.Y. Wu, S.H. Chen, J.I. Chyi, Appl. Phys. Lett. 96 (2010) 123503.
[8] A.S. Shkolnik, E.B. Dogonkin, V.P. Evtikhiev, E. Yu Kotelnikov, I.V. Kudryashov, V.G. Talalaev, B.V. Novikov, J.W. Tomm, G. Gobsch, Nanotechnology 12 (2005) 512.

[9] J. Tatebayashi, B.L. Liang, R.B. Laghumavarapu, D.A. Bussian, H. Htoon, V. Klimov, G. Balakrishnan, L.R. Dawson, D.L. Huffaker, Nanotechnology 19 (2008) 295704.
[10] N.N. Ledentsov, J. Bohrer, M. Beer., F. Heinrichsdorff, M. Grundmann, D. Bimberg, Phys. Rev. B 52 (1995) 14058.
[11] F. Hatami, M. Grundmann, N.N. Ledentsov, F. Heinrichsdorff, R. Heitz, J. Böhrer, D. Bimberg, S.S. Ruvimov, P. Werner, V.M. Ustinov, P.S. Kop'ev, Zh.I. Alferov, Phys. Rev. B 57 (1998) 4635.